Environmental Microbiology (2009) **11**(10), 2585–2597 doi:10.1111/j.1462-2920.2009.01983.x

Viral control of bacterial biodiversity – evidence from a nutrient-enriched marine mesocosm experiment

Ruth-Anne Sandaa,[1]* Laura Gómez-Consarnau,[2] Jarone Pinhassi,[2] Lasse Riemann,[2] Andrea Malits,[3] Markus G. Weinbauer,[3] Josep M. Gasol[4] and T. Frede Thingstad[1]

[1]*University of Bergen, PO Box 7800, Department of Biology, N-5020 Bergen, Norway.*
[2]*Department of Natural Sciences, University of Kalmar, SE-39182 Kalmar, Sweden.*
[3]*Laboratoire d'Océanographie de Villefranche, Université Pierre et Marie Curie Paris VI, UMR 7093, Villefranche-sur-Mer, France.*
[4]*Institut de Ciències del Mar-CSIC. 08003 Barcelona, Catalunya, Spain.*

Summary

We demonstrate here results showing that bottom-up and top-down control mechanisms can operate simultaneously and in concert in marine microbial food webs, controlling prokaryote diversity by a combination of viral lysis and substrate limitation. Models in microbial ecology predict that a shift in the type of bacterial growth rate limitation is expected to have a major effect on species composition within the community of bacterial hosts, with a subsequent shift in the composition of the viral community. Only moderate effects would, however, be expected in the absolute number of coexisting virus–host pairs. We investigated these relationships in nutrient-manipulated systems, under simulated *in situ* conditions. There was a strong correlation in the clustering of the viral and bacterial community data supporting the existence of an important link between the bacterial and viral communities. As predicted, the total number of viral populations was the same in all treatments, while the composition of the viral community varied. Our results support the theoretical prediction that there is one control mechanism for the number of niches for coexisting virus–host pairs (top-down control), and another mechanism that controls which virus–host pairs occupy these niches (bottom-up control).

Received 3 December, 2008; accepted 28 May, 2009. *For correspondence. E-mail ruth.sandaa@bio.uib.no; Tel. (+47) 55584646; Fax (+47) 55589671.

Introduction

Marine viruses are the most numerous biological components of the aquatic environment, with concentrations typically around 10^7 particles ml^{-1} (Bergh *et al*., 1989). Viruses have significant stimulatory and/or inhibitory effects upon microbial biomass and activity, e.g. bacterial abundance and production (Proctor and Fuhrman, 1990; 1992; Suttle, 2005; 2007). Thereby, viral activity affects not only the structure and composition of communities but also modifies the biogeochemical fluxes of matter and energy bypassing particulate matter transport 'up' the food chain to larger organisms, and instead diverting it to dissolved organic matter (DOM) via viral lysis (Bratbak *et al*., 1992; 1994; Fuhrman and Suttle, 1993; Thingstad and Lignell, 1997; Schwalbach *et al*., 2004; Winter *et al*., 2004).

In a hypothetical environment, homogenous in time and space, one could imagine at least two extreme mechanisms for biodiversity control of prokaryotes. Both mechanisms are niche based, in terms of the niche versus neutral theories (Sloan *et al*., 2006). In the bottom-up model each species is present because it has specialized for a given substrate, leading to a system where each species is limited by a different substrate and, thus, organism diversity reflects the diversity of the available substrates (a 'food-specialist' model). The other extreme is a top-down, 'killing the winner' type of mechanism (Thingstad and Lignell, 1997), where selective loss processes like host-specific viral lysis prevent the best competitors from sequestering all the available resources. In such a model, a diverse community of coexisting organisms, all competing for the same resource, is in principle possible. With viral infection being more specific ('species' level) than grazing (which is not species-selective), the total number of organisms in the community would be controlled by grazing, while the loss to lytic viruses would determine the size of each host group and, thus, diversity (Thingstad, 2000). A formalization of this model allows calculation of the number of dominant species, expressed as the ratio between the size of the total community and

the average size of a host group (Thingstad, 2000). While the number of niches in this idealized theoretical scenario is primarily controlled by top-down mechanisms, the ability of a host to occupy one of these niches would depend on the hosts' ability to compete for the limiting substrate(s). Although these models are simple in concept, we are not aware of any experimental data critically testing their predictions.

Several recently published studies have indicated that viral activity has a limited effect on the composition of the bacterial community (Jardillier *et al*., 2005; Hewson and Fuhrman, 2006). Likewise, a recent experimental study (Bouvier and del Giorgio, 2007) has suggested that rare marine bacterial groups are the most susceptible to viral lysis, as these phylotypes might have higher intrinsic activity, higher burst sizes that increase the virus to bacteria ratio, and lower levels of viral resistance, the final result being that they are 'rare'. They also suggest that these rare groups are more effective in resource exploitation, and are thus the winners in nutrient acquisition. Most of the studies concerning the effect of viral activity on the host community have been conducted in manipulated systems using filtration and dilution experiments with virus and virus-free treatments removing all other biological factors, except bacteria, from the sample (Jardillier *et al*., 2005; Hewson and Fuhrman, 2006; Bouvier and del Giorgio, 2007; Zhang *et al*., 2007). In the present study we investigated the relationship between viruses and their hosts under simulated *in situ* conditions.

Our experiment was carried out in nutrient-manipulated systems to study the effect of both top-down and bottom-up control of the bacterial community. A series of mesocosms with coastal north-western Mediterranean water was amended with either glucose (+G), phosphate (+P), both nutrients (+GP) or left un-manipulated (C). The Mediterranean Sea is deficient in phosphate (P) relative to nitrogen (Krom *et al*., 1991; Bethoux *et al*., 1992), and evidence has been found for P-limited bacterial growth dominating in surface waters (Thingstad *et al*., 1998; Van Wambeke *et al*., 2002; Pinhassi *et al*., 2006). Amending such limited water with P, either alone or together with glucose, should therefore create shifts in the limiting factor for bacterial growth, and subsequently result in changes in the composition of the prokaryote and viral communities. The changes in bacterial and viral community structure in the mesocosms and their relationships were monitored using denaturing gradient gel electrophoresis (DGGE) and pulsed field gel electrophoresis (PFGE), respectively, while viral and bacterial abundances were measured by flow cytometry. Our working hypothesis was that changing the type of growth rate limitation of the bacterial community would not substantially affect the number of simultaneously coexisting host–virus pairs, but rather affect the selection for dominant members of the bacterial community, and thus, that viral and bacterial community structure would change in parallel.

Results

Chlorophyll a*, bacterial and viral abundance*

Chlorophyll *a* (Chl *a*) ranged from 0.26 $\mu g\ l^{-1}$ at the beginning of the experiment to an average of 1.33 $\mu g\ l^{-1}$ on day 5 (Fig. 1). In the control treatment the Chl *a* concentration decreased from day 1, while in all other treatments there was an increase with a peak on day 5. This increase was most pronounced in the two P-amended treatments. Nevertheless, addition of glucose alone also resulted in an increase in Chl *a* concentration as compared with the control treatment. The abundance of photosynthetic pico- and nanoeukaryotes generally followed the increase in Chl *a* concentrations, with the highest abundances in P-amended treatments (Fig. S1). The highest abundance of nanoeukaryotes was on day 3 (+G and +GP) and 4 (+P), while the picoeukaryotes peaked in all treatments on day 4 (Fig. S1).

Initial bacterial abundance was around 1.0×10^6 cells ml^{-1} (Fig. 1). In the control treatment abundance increased slightly with a peak on day 4 (1.7×10^6 cells ml^{-1}) and thereafter declined throughout the rest of the experimental period. A small peak in bacterial abundance was also seen in all the other treatments on day 2, with a second peak on day 8 in the two P-amended treatments (+P and +GP). Overall, the average bacterial abundance was the highest in the two P-amended treatments, with the highest abundance in +P on day 8 (3.9×10^6 cells ml^{-1}; Fig. 1).

Total viral abundance was approximately 2.1×10^7 particles ml^{-1} at the start of the experiment and showed no changes in the different treatments until day 2 (Fig. 1). From day 2 there was a major increase in the number of viral particles both in the +GP and in the +P treatments, while only minor changes were seen in the control and +G treatments. The increase in viral abundance was the highest in the +GP treatment, compared with the control, reaching an average of 1.4×10^8 particles ml^{-1} on day 8 while the corresponding number in the +P treatment was 8.2×10^7 particles ml^{-1} (Fig. 1).

Bacterial community dynamics

The DGGE analysis showed that bacterial community composition changed over time and responded to the different treatments (Fig. 2A and B). By cluster analysis of the DGGE profiles, a dendrogram consisting of three main clusters was produced (Fig. 4A). Samples from day 0 made up one cluster (I) together with one sample from the

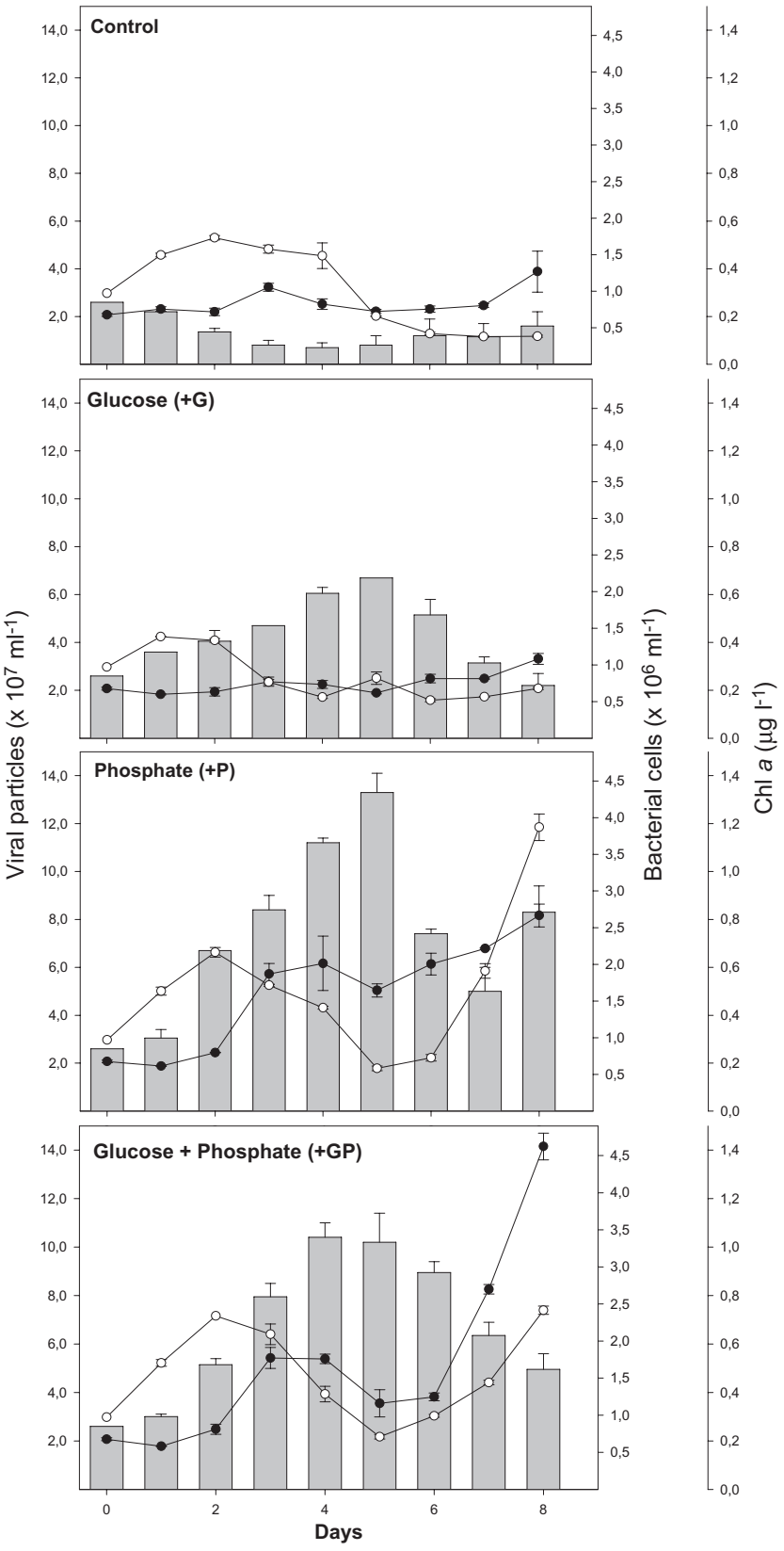

Fig. 1. Development of total viral (solid circle) and bacterial (open circle) abundances and Chl *a* (bars) in the different treatments. Values are mean and ranges of two replicate tanks.

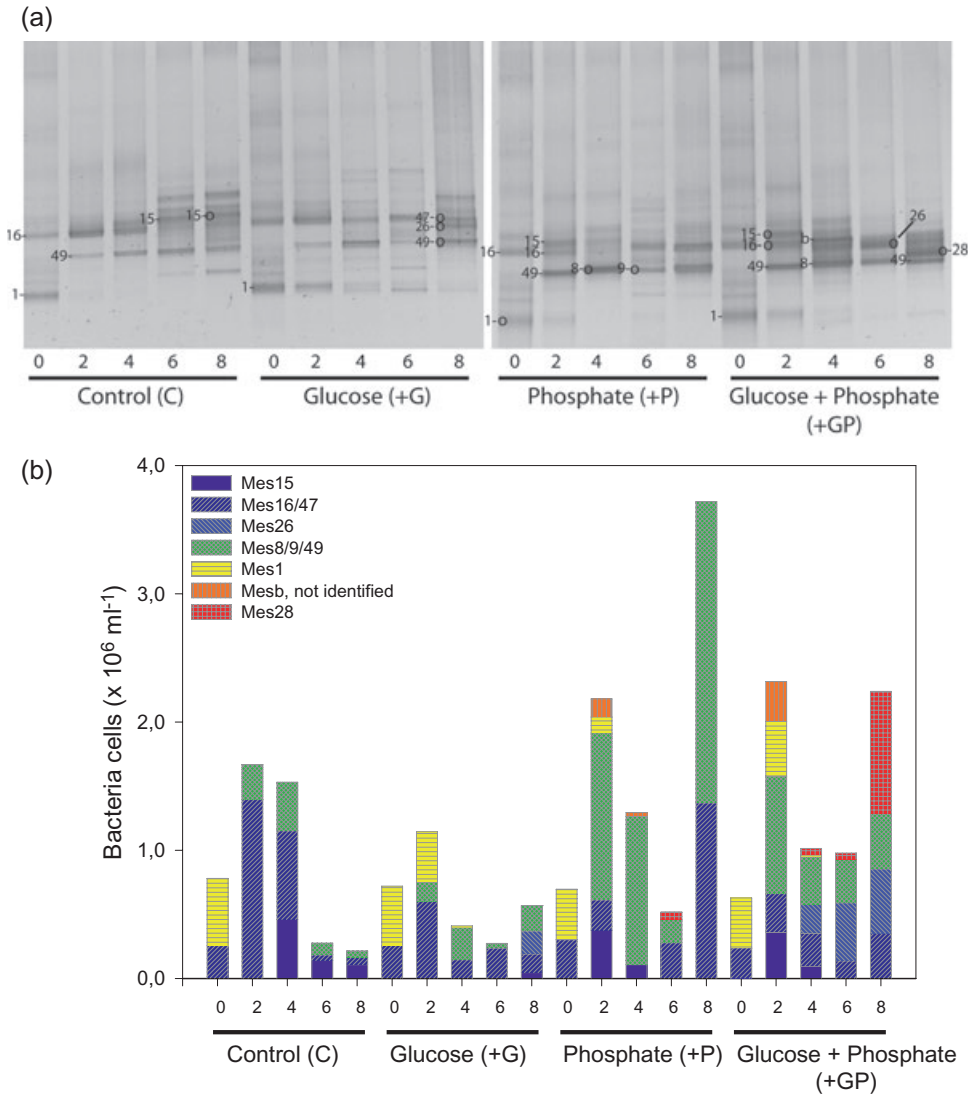

Fig. 2. A. Bacterioplankton composition during the mesocosm experiment as determined by DGGE of PCR-amplified partial 16S RNA genes. Circles denote the exact bands that were sequenced. Numbers refer to phylotype number. Several identical numbers have been inserted to facilitate visual identification of vertically aligned bands. Day of sampling and treatment is given below each lane.
B. Stacked bar plot of the most dominant bacterial phylotypes. The relative intensity of each band was multiplied by total bacterial abundance and we only show the phylotypes that are estimated to have exceeded at least once 200 000 cells ml^{-1} following this calculation.

+G treatment (day 2). Cluster II consisted of samples from the C and +G treatments, with two exceptions (+P treatment days 6 and 8). The third cluster consisted of samples from the +P and +GP treatments, except for two samples, one from the +G treatment (day 8) and one from the +C treatment (day 2).

Since virus infection is dependent on the density of hosts we focused our analysis on the numerically dominant bacterial phylotypes. These were putatively identified by scaling the relative contribution of each band to total intensity in each lane to total bacterial abundance. Phylotypes which sometime during the experiment exceeded an arbitrary estimated threshold in relative abundance of 200 000 cells ml^{-1} were defined as dominant (Fig. 2B). Except for Mes1 (*Synechococcus*), which was seen in all treatments at the beginning of the experiment, all dominant DGGE phylotypes belonged to the *Roseobacter* group (Table 1). A pronounced temporal and between-treatment variation in the abundance of individual phylotypes was observed. Two groups of dominant bands were present in all treatments practically all through the experiment (Mes16/Mes47, and Mes8/Mes9/Mes49). These were the only dominant bands in the +P treatment on day 8. Mes15 made a short appearance on day 2 in the +P and the +GP treatments, but was also detected in the other treatments. Mes26 was detected in both the +G and +GP treatments, while the unidentified band, Mesb, was detected in all treatments in the beginning of the

Table 1. Relationship of excited DGGE band sequences (phylotypes) to other sequences in GenBank.

Phylotype	Accession No.	Closest matching entry in GenBank	Accession No. (closest match)	Similarity (%)
Mes1	EF441554	Uncultured bacterium clone PDM-OTU8	AY700638	100
		Synechococcus sp. WH 8109	AY172836	100
Mes8	EF441555	Uncultured alphaproteobacterium clone JL-ECS-X8	AY663968	99
		Jannaschia cystaugens	AB121782	96
Mes9	EF441556	Uncultured *Roseobacter* sp. clone ST-13	AY573530	100
		Roseobacter gallaeciensis	AY136134	97
Mes15	EF441558	Uncultured alphaproteobacterium clone PI_4a9f	AY580451	98
		Roseobacter gallaeciensis	AY136134	96
Mes16	EF441559	Marine arctic deep-sea bacterium HD9	AJ557871	98
		Agrobacterium gelatinovorum	D88523	96
Mes26	EF441561	*Agrobacterium gelatinovorum*	D88523	98
		Thalassobacter oligotrophus	AJ631302	98
Mes28	EF441562	*Roseobacter* sp. JL-126	AY745859	98
		Alphaproteobacterium MBIC1887	AB026492	98
Mes47	EF441568	*Roseobacter* sp. HYL-SA-18	DQ008594	97
		Agrobacterium gelatinovorum	D88523	97
Mes49	EF441570	*Rhodobacteraceae* bacterium CL-TA03	AY962292	97
		Jannaschia cystaugens	AB121782	96

experiment. Mes28 was the most dominant band on day 8 in the +GP treatment (Fig. 2B).

Viral community dynamics

The PFGE analysis showed that the viral community also changed over time and responded to the different treatments (Fig. 3A). This was particularly evident from the cluster analysis of the PFGE fingerprints, resulting in a dendrogram consisting of two groups. Group I contains samples from the +G and C treatments while group II consists of samples from the +GP and +P treatments (Fig. 4B). A total of 23 viral populations were detected during the experimental period with genome sizes ranging from 30 to 560 kb (Fig. 3A). There was an increase in the number of viral populations from 5 on day 0 to a maximum of 13 viral populations on day 6 (+G treatment) (Fig. 3B). The total numbers of viral populations in the +GP and +P treatments and in the C and +G treatments were, however, relatively similar (Fig. 3B), despite differences in the genome size distribution (Fig. 3A). All samples comprised viral populations in the size range from 30 to 194 kb, and seven of these were present in all treatments (Fig. 3A, black dots). The C and +G treatments comprised seven additional bands (Fig. 3A, red dots), while the +GP and +P treatments comprised eight additional bands, all in a smaller genomic size range (Fig. 3A, green dots). One population of 48 kb was only detected in the +G and +P samples on day 6 and 8 (Fig. 3A, blue dots). The number of bands with different genome sizes between 30 and 195 kb was nearly twice as high in the samples from the +GP and +P treatments (16 different genome sizes) compared with the C and +G treatments (eight different genome sizes) (Fig. 3A).

The Mantel test showed a strong, significant correlation between the bacterial and viral clustering ($r = 0.924$, and $P < 0.001$) indicating that the changes produced by the treatments in bacteria were similar to those occurring in the viruses.

Discussion

Two models, based on two ecological theories 'the neutral theory' and 'the niche partitioning', have recently been discussed for describing the shapes of prokaryotic communities (Sloan *et al*., 2006; Battin *et al*., 2007). The neutral theory (Hubbell, 2001) explains diversity and relative abundance of species in that the differences between members of an ecological community of trophically similar species are neutral, or irrelevant to their success (Battin *et al*., 2007). This is in contrast to the traditional niche theory that suggests that environmental factors and competition for resources drive the differentiation of species by natural selection. In the present study we have shown that both top-down (by virus lysis) and bottom-up forces will act in concert shaping prokaryote community structure. Our observations suggest that these mechanisms are niche-based in terms of the above definitions (Sloan *et al*., 2006). Before we expand this discussion, there are a few elements of the results worth commenting.

Effect of nutrient limitations

As anticipated from previous research (see *Introduction*), the microbial community in the sampled Mediterranean surface waters appeared P-starved at the start of the experiment. This was suggested by clear increases in

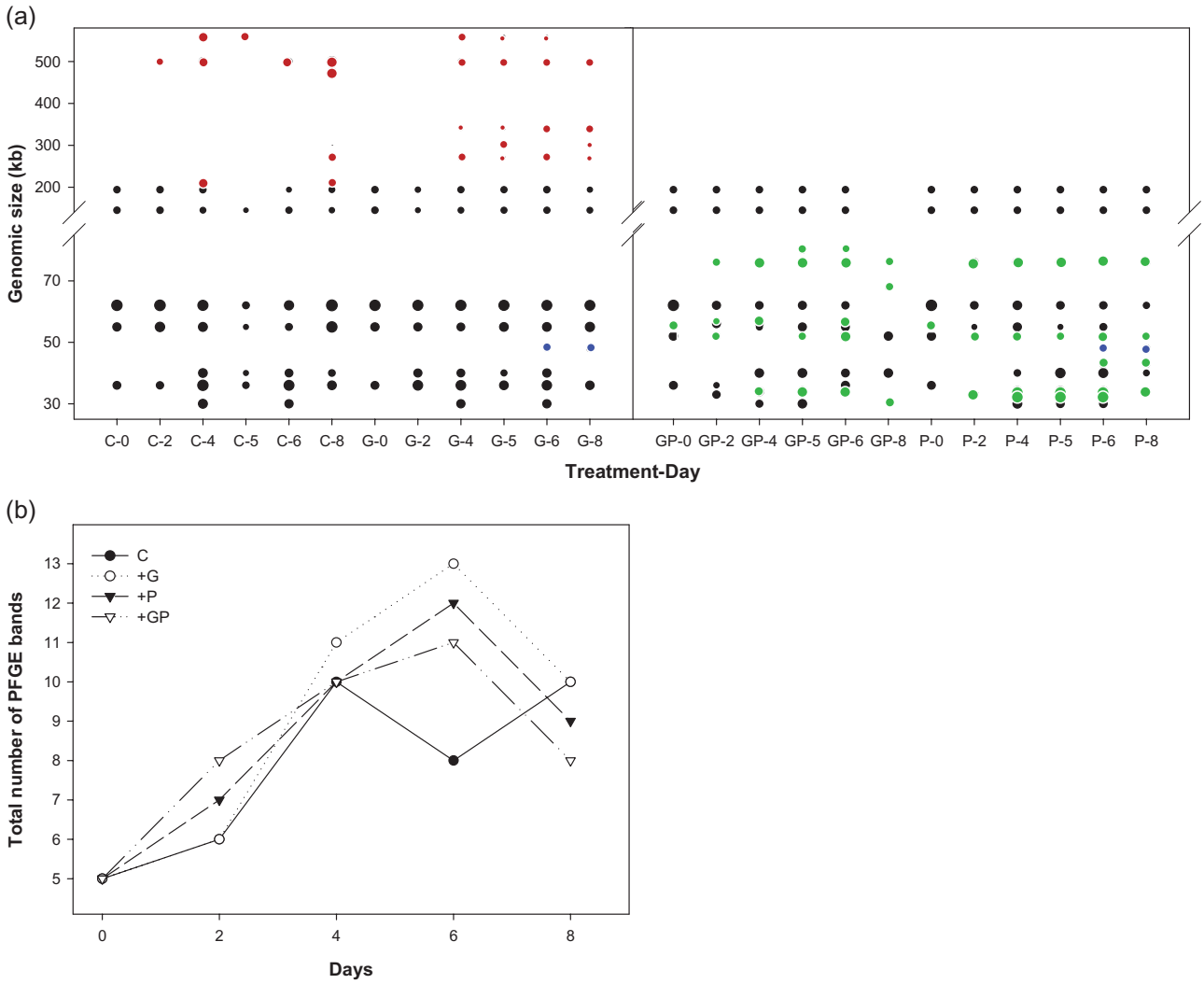

Fig. 3. Viral community structure during the mesocosm experiment as determined by PFGE.
A. Schematic outline of the viral populations defined by genome size. The outline is based on three different electrophoresis runs for each viral sample. Red dots: viral populations present in the control and glucose (+G) treatments. Green dots: viral populations present in the phosphate (+P) and glucose and phosphate (+GP) treatments. Blue dots: viral populations present in the +G and +P treatments. The size of the dots represents the intensity of the PFGE bands. Letters indicate treatments; numbers indicate days of sampling.
B. Numbers of different viral populations (PFGE bands) over time in the different treatments.

particulate P, bacterial production (Tanaka *et al*., in press) and Chl *a* in the P-amended treatments (+P and +GP), as well as by the lack of any stimulatory effect of glucose on bacterial abundance in the +G treatment. Unexpectedly, the addition of glucose alone (+G) had a positive effect on Chl *a* levels and a slightly negative effect on bacterial abundance. One may speculate that in this experiment, performed with relatively low artificial illumination, light (energy) may have been limiting for phytoplankton growth. Phytoplankton species able to use the excess glucose as additional energy source could then in principle improve their competitive ability for the limiting phosphate, competing favourably against bacteria (Lewitus and Kana, 1994).

Bacterial community dynamics

Changes in the bacterial community were most pronounced in the treatments with addition of phosphate. One of these effects was cell number being five and eight times higher in the +P and +GP treatments, respectively, compared with the control and the +G treatments. The bacterial community was dominated by *Alteromonas* and *Roseobacter*. These bacteria formed > 50% of total bacterial counts (Allers *et al*., 2007). In the first days of the experiment there was a bloom of *Alteromonas* in all treatments, followed by a pronounced bloom of *Roseobacter* in the +P and +GP treatments. Our DGGE analysis also shows differences within the *Roseobacter* group between

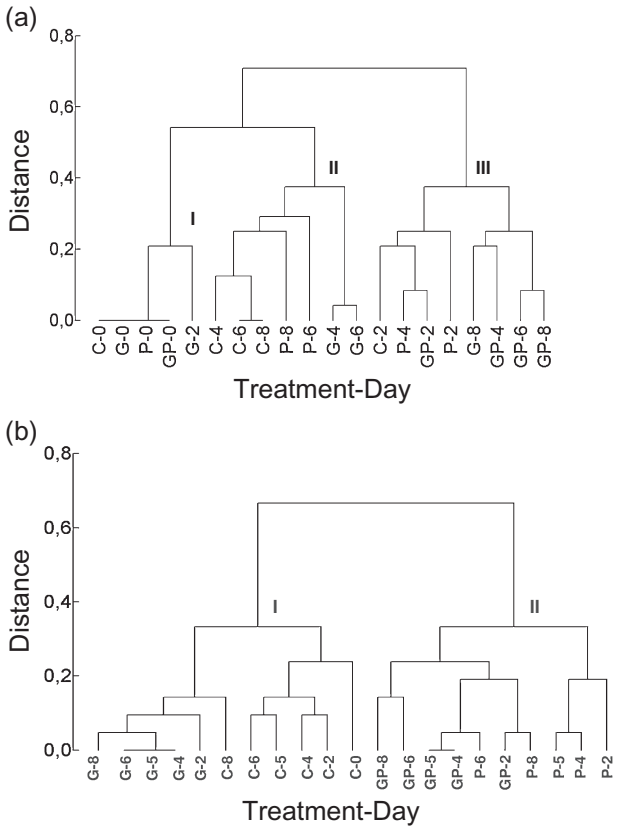

Fig. 4. Cluster analysis of the DGGE (A) and PFGE (B) fingerprints. First letters indicate treatment; numbers indicate the day of sampling.

treatments, indicating that different members of this group were differentially affected by the different nutrient availability. For example, the phylotype Mes28 was seen as a very dominant band in the +GP treatment on day 8. Another phylotype, Mes26, was only detected in the +G (day 8) and +GP treatments (day 4–8). This suggests that these single phylotypes have special preferences for growth with higher +G or +GP concentrations respectively.

The DGGE bands belonging to *Roseobacter* and *Synechococcus* showed similar dynamics as the abundance of these bacterial groups determined by FISH (Allers *et al*., 2007) or by flow cytometry (Fig. S2). Phylotype Mes1 (*Synechococcus* sp.) disappeared on day 4 from all treatments except from the control, simultaneous with a sharp decrease in flow-cytometrically determined *Synechococcus* abundance (Fig. S2). Similar trends were seen for *Roseobacter*, where there was an increase during the experimental period both in the intensity of bands belonging to the *Roseobacte*r group and in the abundance of *Rhodobacteriaceae* cells enumerated by CARD-FISH (Allers *et al*., 2007). The DGGE analysis is based on PCR-amplified products, a technique known to potentially introduce biases (Wintzingerode *et al*., 1997). The quantitativiness of PCR has been disputed, and the prevailing view is that the intensity of the DGGE bands cannot be used as a precise measurement of the abundance of the organisms represented by the bands. One reason is that dominant templates may be evened out in the final PCR product (Suzuki and Giovannoni, 1996). Consequently analyses of products of end-point PCRs, as in the present study, may falsely suggest a high number of co-dominant phylotypes. Nevertheless, several studies have shown that DGGE band intensity may be used as a rough estimate of the relative abundance of phylotypes (Riemann *et al*., 1999; Casamayor *et al*., 2000). Thus, in our study we combined the relative intensity of the DGGE bands with cell counts to compensate for variations in total bacterial abundance during the experiment. Hence, the relative contribution of phylotypes, e.g. *Roseobacter*, to the bacterial community is reported as a cell number in relative terms (Fig. 2B).

Bacteria became more P-limited during the first 3 days of the experiment (Tanaka *et al*., in press), and this was accompanied by a change in bacterial community structure, for example, with the occurrence of one phylotype (Mes8/9/49), belonging to the *Roseobacter* group. This phylotype was present in all treatments from day 2 until the end of the experiment, becoming most dominant in the +P and +GP treatment. Interestingly, this phylotype became less dominant in the P treatment on day 6, for thereafter to increase in abundance again on day 8. Specific phosphate affinity, defined as specific phosphate uptake rate corrected for the biomass of phytoplankton and bacterial community, has been used to determine the available phosphate pool for osmotrophs (Tanaka *et al*., 2006). Specific phosphate affinity measured in parallel with this study suggested an increase from day 5 followed by a decrease of the available phosphate pool in the +P treatment on day 8 (Tanaka *et al*., in press). Thus, the presence of these phylotypes might be coupled to a different extent of P limitation, or to viral lysis as discussed below. Few studies have focused on investigating whether microdiversity in the 16S rRNA gene is related to variability in phenotypic properties (Acinas *et al*., 2004; Selje *et al*., 2004). Our data suggest that the different members of the *Roseobacter* group could have different growth requirements for P or as mentioned above, special preferences for glucose, while having relatively similar 16S rRNA gene sequences.

Viral community dynamics

Addition of phosphate resulted in a major change in viral community structure as compared with the control, while addition of glucose had only minor effects. This was clearly shown by approximately a doubling in the abundance of viral populations with genome sizes

< 190 kb from day 5 in the +P and +GP treatments compared with the C and +G treatments. A similar effect was seen on total viral abundance, with approximately two and four times higher counts in the +P and +GP treatments, respectively, on day 8, compared with the control. The viral assemblage was distributed in a genome size range from approximately 20–560 kb, with the most dominant populations in the genome size range 20–100 kb. This is congruent with the genome size range of most cultured marine bacteriophages with dsDNA genomes (Ackermann and DuBow, 1987; Jiang *et al*., 2003).

Another major difference in the viral communities between treatments was the presence of viral populations with genome sizes in the range 210–500 kb in the C and +G treatments. These genomes were absent from the +P and +GP treatments. Viruses infecting pico- and nanoeukaryotic phytoplankton have genomes in this size range (Van Etten and Meints, 1999; Sandaa *et al*., 2001; Castberg *et al*., 2002). However, the numbers of pico- and nanoeukaryotes were the lowest in the samples from the C and +G treatments (below 6×10^3 and 80 cells ml^{-1} respectively) (Fig. S1), showing no correlation with these large genome-sized viral populations. One explanation might be that these large genome-sized viruses in fact do infect pico- and nanoeukaryotes but that high lysis rate and/or large burst size (Sandaa *et al*., 2001) lead to a continuous presence of these viruses after a decline in the numbers of the hosts.

Virus–host dynamics and the effect on host diversity

Theories have been put forward that imply viruses to have an effect on the species richness of the bacterial community (Thingstad and Lignell, 1997). To our knowledge no empirical evidence based on *in situ* experiments exists, as most of the studies concerning the effect of viral activity on the host community have been conducted in manipulated systems where they have compared virus-containing and virus-free treatments removing all other biological factors, except bacteria, from the sample (Jardillier *et al*., 2005; Hewson and Fuhrman, 2006; Bouvier and del Giorgio, 2007; Zhang *et al*., 2007; Pradeep Ram and Sime-Ngando, 2008). In our study, several links between viruses and their hosts were detected under simulated natural conditions. Phosphate addition, either alone or together with glucose, produced the most pronounced change in the structure of both bacterial and viral communities relative to the control. A similar link was also seen in viral and bacterial abundance, where peaks in bacterial abundance were generally followed by increases in viral abundance. Further, only minor changes in viral and bacterial community structures and dynamics were seen when glucose was added alone. A similar effect of phosphate addition on the prokaryote and hence the viral community under P-limiting conditions was newly demonstrated in a freshwater microcosm study by Pradeep Ram and Sime-Ngando (2008). Of the different amendments, addition of P resulted in the most pronounced effect on the prokaryote and viral community shown by an increase in prokaryotic abundance, production and growth efficiency, compared with the unamended controls. This change resulted in an increase in the viral abundance, production and viral-induced lyses of the prokaryotes (Pradeep Ram and Sime-Ngando, 2008), also supporting a tight coupling between viruses and their hosts. Another plausible link between viruses and their hosts in our study could be represented by the oscillation seen in different bacterial phylotypes. One phylotype (Mes8/9/49), belonging to the *Roseobacter* group, was present in all treatments from day 2 until the end of the experiment, becoming most dominant in the +P and +GP treatment. This phylotype became less dominant in the P treatment on day 6, thereafter to increase in abundance again on day 8. Such oscillation may be explained by phylotypes being lysed by their specific phage, thereby enabling another genotypically related phylotype to occupy its niche. This would lead to Lotka-Volterra oscillation of the phylotypes and their specific phages as proposed by the Killing-the-Winner hypothesis (Thingstad and Lignell, 1997) but also support the niche partitioning theory in that a small number of species interact through fixed rules (Chave, 2004). Using DGGE and PFGE to study shifts in the composition of the bacterial and viral community structure, Riemann and Middelboe (2002) found the same pattern to be stable over spatial and temporal scales while pattern changes were seen when crossing hydrographical fronts. Using the same techniques, Øvreas and colleagues (2003) demonstrated in mesocosm experiments that manipulations were found to have similar effects on both types of band patterns indicating similar changes in both communities. These observations support our results showing a co-variation between shifts in the composition of the bacterial and viral community structure.

The changes generated by the different treatments were most pronounced in the viral community, where the PFGE samples clustered into two distinct groups, with or without P addition. This grouping was not as evident in the DGGE samples, where several clusters contained samples from different treatments. Viruses are clearly but indirectly influenced by the nutrient limitation, which can directly control the resource for viruses, their hosts (Weinbauer *et al*., 2003). Thus, viruses only respond to changes in host organisms induced by environmental differences as viruses themselves cannot take up or process chemical changes. As the decay rate for viruses is relative high (up to 1.1 h^{-1}; Heldal and Bratbak, 1991), changes seen in viral community structure must reflect recent changes in host community structure. According to the niche model,

different limiting substrates are expected to select for different compositions of host communities, and corresponding differences in the composition of the phage communities should be expected. If, however, there is a trade-off between competitive ability in terms of nutrient uptake and defence ability against viral infection (Thingstad, 2000), fast-growing competition specialists (r-strategists) would presumably be the least abundant, while their associated viral populations would have the highest abundances. Further, the defence specialists (K-strategists), being more or less immune to viral attack, would grow slowly, but be more abundant and have an associated viral population maintained at low abundances. If we interpret our results based on this theory, the dominating common DGGE bands in the different treatments would represent defence specialists (K-strategists), resisting phage attack, while the changes in the number of viral populations (> 190 kb genomes) may represent bacteriophages lysing fast-growing competition specialists (r-strategists). Interestingly, one of the suggested viral r-strategists, the T7-like *Podoviridae* (Suttle, 2007), was indeed one of the dominant phage groups in this experiment (R.-A. Sandaa, unpubl. results).

While pronounced changes were seen in viral community structure due to the different treatments, the number of viral populations (PFGE bands) was, nevertheless, the same in all treatments. Thus, as hypothesized, changes in the growth rate limitation of the bacterial community did not produce dramatic effects in the number of simultaneously coexisting host–virus pairs, but rather selected for specific members of the bacterial community. This expectation is based on the concept that competition under different types of limitation requires different cell properties, and thus selects for different hosts. As a result, also the composition of the corresponding viral community would be expected to change.

The 16S rDNA DGGE analysis did not support the assumptions about similar numbers of coexisting host–virus pairs in the different treatments, based on number of bacterial phylotypes detected (Fig. S3). This might be due to limitations in the DGGE method. Due to heterogeneity of 16S rDNA (Fogel *et al*., 1999), one bacterial species might produce several bands when separated on a DGGE gel (Dahllof *et al*., 2000). In addition, dissimilar sequences may co-migrate to the same position in a DGGE gradient (Muyzer *et al*., 1998). Thus, it is difficult to interpret the number of bacterial species in a sample based on the number of DGGE bands. Congruently, the PFGE method does not discriminate between different viral types with similar genome sizes. Nevertheless, a similar dynamic in the number of viral populations was seen between the different treatments.

The effects of nutrient treatments were detected in both the host and viral populations, although the effect was most pronounced in the viral community. Thus, our data support the speculations that viral infection may affect a few abundant host phylotypes, whereas other phylotypes could be resistant to infections (Schwalbach *et al*., 2004; Jardillier *et al*., 2005; Holmfeldt *et al*., 2007). The alterations of the bacterial community could therefore result at first from viral lysis of phylotypes that are good competitors for nutrients, and then from interspecific competition for resources by virus-resistant phylotypes that are less efficient competitors for nutrients. In addition, the results support our hypothesis that changes in the chemical environment in a manner that switches the bacterial community to another type of growth rate limitation do not result in dramatic effects on the number of simultaneously coexisting host–virus pairs, but rather shift the selection for dominant members of the bacterial community. Consequently, the composition of the corresponding viral community also changes. Taken together, this would suggest that top-down regulation (by virus infection) and bottom-up regulation (by nutrient availability) both play key roles in shaping bacterioplankton community composition in aquatic environments. In more general terms our results demonstrate the relationship between bottom-up and top-down control on population dynamics, community structure and evolutionary change.

If evaluated within the frameworks of the neutral and niche theories, our results suggest that the prokaryotic communities are regulated by forces that can be explained only by the niche theory. The methods we have applied in the present study may not be sensitive enough to capture the full diversity at the species level. Still our results do demonstrate a link between changes in the structure of the prokaryote community and changes seen in the viral community. Nevertheless, in microbial ecology, top-down processes will include both specific viral lysis and grazing by protozoans. In our study, heterotrophic nanoflagellates (HNF) did peak in number after a decline in the bacterial number (Allers *et al*., 2007). This indicates that top-down regulation by grazing could not be neglected as a possible mortality factor in this experiment. Both specific viral lysis and grazing by protozoans have been shown to result in roughly equal losses (~40%) of prokaryotes in marine systems (Suttle, 1994; Fuhrman and Noble, 1995). It has been emphasized that neutral and niche theories are complementary, not conflicting (Chave, 2004; Leibold, 2008), and that both may be used to explain different aspects of biodiversity (Kelly *et al*., 2008). As mentioned, in a simplified model, top-down control by viral lysis may be understood by the niche partitioning theory. The process is specific by selective lysis of host populations. This will have a strong bottom-up effect because lysis alters the quality and quantity of growth-limiting resources (Brussaard *et al*., 2008). Grazing of prokaryotes by protozoans is, in principle,

stochastic; thus, it might be described more accurately by the neutral model. In general, it would imply that the regulation of the total number of prokaryotes in a community shows neutral dynamics, whereas the size of each host group, e.g. the diversity, is determined by niche partitioning.

Experimental procedures

Mesocosm set-up and sampling

Water was collected from 1 m depth at the Blanes Bay Microbial Observatory in the Catalan coast (NW Mediterranean, 40°40′N, 2°48′E) on 19 October 2004. The water was transported to the laboratory and filled into 200 l tanks. The tanks were maintained at *in situ* temperature (20°C) with relatively low light (average 100 μE m^{-2} s^{-1}) on a 12:12 h light : dark cycle. All tanks, including the controls, received 2 μM NH_4Cl daily in order to prevent N limitation. Additionally, mesocosms were amended daily with 50 nM PO_4 (KH_2PO_4) (treatment designation +P), with 13.25 μM glucose (treatment designation +G) or with both glucose and PO_4 at the same concentrations as in the separate additions (treatment +GP). The treatments were set up in duplicates and monitored for a total of 8 days. All mesocosms were mixed twice a day by hand-held stirring, and samples were taken each morning before nutrients were added. Samples for viral and bacterial counts and Chl *a* measurements were collected from both series every day. The samples for DGGE and PFGE were collected from one of the series every second day. Samples for PFGE were in addition collected on day 5.

Viral and bacterial counts

Total number of bacteria and viruses were determined with a Becton & Dickinson FACSCalibur flow cytometer (BD Bioscience, Franklin Lakes, NJ, USA). For bacteria, samples of 1 ml were fixed with 1% buffered paraformaldehyde solution (PFA, pH 7.0) plus 0.05% glutaraldehyde, incubated for 10 min at room temperature, then stored in liquid nitrogen. Two hundred microlitres of these samples were stained for 10 min with SybrGreen I (Molecular Probes, Eugene, OR, USA). For flow cytometric concentration determination, 10 μl of a solution of yellow-green latex beads (size, 1 μm; final concentration, 10^6 ml^{-1}; Polysciences, Washington, PA, USA) was added to each sample as an internal standard and the bacterial cell numbers were determined from the ratios of cells to beads.

For viruses, samples of 2 ml were fixed with 0.5% glutaraldehyde, incubated for 15 min at 4°C, flash-frozen in liquid nitrogen and stored at −80°C until analysis. Each sample was diluted 100-fold with TE buffer (10 mM Tris, 1 mM EDTA, pH 8) before they were stained with SYBR Green I (Molecular Probes). The flow cytometer instrumentation and the remaining methodology followed the recommendations of Brussaard (2004). Abundances were calculated from the measured flow rate.

Chlorophyll a

Concentrations were determined following standard procedures. Subsamples of 150 ml were filtered through GF/F glass fibre filters and subsequently extracted overnight at 4°C in 90% acetone. Fluorescence of the extracts was measured with a Turner designs fluorometer.

Bacterial community dynamics

Analysis of bacterial community composition and dynamics in this experiment has been published recently (Allers *et al*., 2007) where population dynamics of *Alteromonas* and *Roseobacter* were examined by DGGE and CARD-FISH. In the present study we perform further analyses of bacterial community dynamics and examine the potential linkage to changes in viral community structure. Thus, the procedures for DNA extraction, PCR and DGGE are only briefly outlined here.

Microbial biomass from ~700 ml of sample was collected onto 0.2-μm-pore-size polycarbonate filters (Durapore, Millipore). Filters were stored frozen at −70°C in sucrose buffer (0.75 M sucrose, 40 mM EDTA, 50 mM Tris pH = 8.3) until DNA extraction (Allers *et al*., 2007). Partial bacterial 16S rRNA genes were PCR amplified using primers GC341F (Muyzer *et al*., 1993) and 907RM (Muyzer *et al*., 1998). Excised DGGE bands were sequenced (Allers *et al*., 2007) and compared with existing prokaryotic sequences in GenBank (NCBI) using BLAST (Altschul *et al*., 1990). Sequences were submitted to GenBank with Accession No. Mes1, EF441554; Mes8, EF441555; Mes9, EF441556; Mes15, EF441558; Mes16, EF441559; Mes26, EF441561; Mes28, EF441562; Mes47, EF441568; Mes47, EF441570 (Table 1, Allers *et al*., 2007).

Viral community dynamics

Virus particles from 5 l of sample were concentrated down to 35 ml using a Vivaflow 200 tangential flow module with a cut-off of 100 000 MWCO (Vivascience, Lincon, UK) following the manufacturer's procedure. The concentrate was clarified by centrifugation in a swing-out centrifuge (Beckmann J2-HS), twice at 7000 *g* for 30 min at 4°C. Viral particles were subsequently concentrated by ultracentrifugation (Beckman L8-M with SW-28 rotor) for 2 h at 28 000 r.p.m. at 10°C. The viral pellet was dissolved in 200 μl of SM buffer (0.1 M NaCl, 8 mM $MgSO_4 \cdot 7H_2O$, 50 mM Tris-HCl, 0.005% w/v glycerine).

Four viral agarose plugs were prepared from the 200 μl viral concentrate for PFGE. The samples were run on a 1% w/v SeaKem GTG agarose (FMC, Rockland, Maine) gel in 1× TBE gel buffer using a Bio-Rad DR-II CHEF Cell (Bio-Rad, Richmond, CA, USA) electrophoresis unit. From each sample we used three of the plugs and ran them at three different pulse-ramp conditions in order to separate a large range of viral genome sizes (Sandaa and Larsen, 2006). Gels were visualized and digitized using the Fujifilm imaging system, LAS-3000.

Statistical analyses of bacterial and viral community composition

Digitized DGGE images were analysed with the Quantity-one software (Bio-Rad). The software allows identification of

different bands and calculation of the contribution of each band to total band intensity in each lane. The PFGE banding patterns were analysed using the computer program GEL2K (Svein Norland, UoB, Norway), which calculates the molecular weight of the different DNA fragments, the intensity of each of the DNA fragments, and determines the presence or absence of bands. The resultant matrix of both DGGE and PFGE was used for cluster analysis using the GEL2K program. Clustering was based on simple matching algorithm, while the dendrogram was drawn using the complete link method. The significance of the correlation between the two matrices in the two data sets was tested by using the free software program ZT version 1.1 (http://www.psb.ugent.be/~erbon/mantel/; Bonnet and Van de Peer, 2002) by running simple Mantel test (Mantel, 1967) with 100 000 permutations.

Acknowledgements

We thank Vanessa Balagué and Clara Cardelús for analyses of chlorophyll, and Jordi Felipe, Philippe Catala and Philippe Lebaron for the bacterial abundance determinations. We also thank Rafel Simó, Maria Vila-Costa, Ramon Massana and the rest of the participating scientists for their help in mesocosm set-up and sampling. This study was performed with financial support from the EU project BASICS (EVK3-CT-2002-00078), the Research Council of Norway projects: Pame-Nor 'DOC turnover in polar microbial food webs' and VIPMAP (186142).

References

Acinas, S.G., Klepac-Ceraj, V., Hunt, D.E., Pharino, C., Ceraj, I., Distel, D.L., and Polz, M.F. (2004) Fine-scale phylogenetic architecture of a complex bacterial community. *Nature* **430:** 551–554.

Ackermann, H.-W., and DuBow, M.S. (1987) *Viruses of Prokaryotes*. Boca Raton, FL, USA: CRC Press.

Allers, E., Gómez-Consarnau, L., Pinhassi, J., Gasol, J.M., Šimek, K., and Pernthaler, J. (2007) Response of *Alteromonadaceae* and *Rhodobacteriaceae* to glucose and phosphorus manipulation in marine mesocosms. *Environ Microbiol* **9:** 2417–2429.

Altschul, S., Gish, W., Miller, W., Myers, E., and Lipman, D. (1990) Basic local alignment search tool. *J Mol Biol* **215:** 403–410.

Battin, T.J., Sloan, W.T., Kjelleberg, S., Daims, H., Head, I.M., Curtis, T.P., and Eberl, L. (2007) Microbial landscapes: new paths to biofilm research. *Nat Rev Microbiol* **5:** 76–81.

Bergh, O., Borsheim, K.Y., Bratbak, G., and Heldal, M. (1989) High abundance of viruses found in aquatic environments. *Nature* **340:** 467–468.

Bethoux, J.M.P., Madec, C., and Gentili, B. (1992) Phosphorus and nitrogen behaviour in the Mediterranean Sea. *Deep Sea Res Part A* **39A:** 1641–1654.

Bonnet, E., and Van de Peer, Y. (2002) ZT: a software tool for simple and partial Mantel tests. *J Statistical Software* **10:** 1–12.

Bouvier, T., and del Giorgio, P.A. (2007) Key role of selective viral-induced mortality in determining marine bacterial community composition. *Environ Microbiol* **9:** 287–297.

Bratbak, G., Heldal, M., Thingstad, T.F., Riemann, B., and Haslund, O.H. (1992) Incorporation of viruses into the budget of microbial C-transfer – a 1st approach. *Mar Ecol Prog Ser* **83:** 273–280.

Bratbak, G., Thingstad, F., and Heldal, M. (1994) Viruses and the microbial loop. *Microb Ecol* **28:** 209–221.

Brussaard, C.P.D. (2004) Optimization of procedures for counting viruses by flow cytometry. *Appl Environ Microbiol* **70:** 1506–1513.

Brussaard, C.P.D., Wilhelm, S.W., Thingstad, F., Weinbauer, M.G., Bratbak, G., Heldal, M., *et al.* (2008) Global-scale processes with a nanoscale drive: the role of marine viruses. *ISME J* **2:** 575–578.

Casamayor, E.O., Schafer, H., Baneras, L., Pedros-Alio, C., and Muyzer, G. (2000) Identification of and spatio-temporal differences between microbial assemblages from two neighboring sulfurous lakes: comparison by microscopy and denaturing gradient gel electrophoresis. *Appl Environ Microbiol* **66:** 499–508.

Castberg, T., Thyrhaug, R., Larsen, A., Sandaa, R.A., Heldal, M., Van Etten, J.L., and Bratbak, G. (2002) Isolation and characterization of a virus that infects *Emiliania huxleyi* (Haptophyta). *J Phycol* **38:** 767–774.

Chave, J. (2004) Neutral theory and community ecology. *Ecol Lett* **7:** 241–253.

Dahllof, I., Baillie, H., and Kjelleberg, S. (2000) rpoB-based microbial community analysis avoids limitations inherent in 16S rRNA gene intraspecies heterogeneity. *Appl Environ Microbiol* **66:** 3376–3380.

Fogel, G.B., Collins, C.R., Li, J., and Brunk, C.F. (1999) Prokaryotic genome size and SSU rDNA copy number: estimation of microbial relative abundance from a mixed population. *Microb Ecol* **38:** 93–113.

Fuhrman, J.A., and Noble, R.T. (1995) Viruses and protists cause similar bacterial mortality in coastal seawater. *Limnol Oceanogr* **40:** 1236–1242.

Fuhrman, J.A., and Suttle, C.A. (1993) Viruses in marine planktonic systems. *Oceanography* **6:** 51–63.

Heldal, M., and Bratbak, G. (1991) Production and decay of viruses in aquatic environments. *Mar Ecol Prog Ser* **72:** 205–212.

Hewson, I., and Fuhrman, J.A. (2006) Viral impacts upon marine bacterioplankton assemblage structure. *J Mar Biol Assoc UK* **86:** 577–589.

Holmfeldt, K., Middelboe, M., Nybroe, O., and Riemann, L. (2007) Large variability in host strain susceptibility and phage host-range govern interactions between lytic marine phages and their flavobacterium hosts. *Appl Environ Microbiol* **73:** 6730–6739.

Hubbell, S.P. (2001) *The Unified Neutral Theory of Biodiversity and Biogeography*. Princeton, NJ, USA: Princeton University Press.

Jardillier, L., Bettarel, Y., Richardot, M., Bardot, C., Amblard, C., Sime-Ngando, T., and Debroas, D. (2005) Effects of viruses and predators on prokaryotic community composition. *Microb Ecol* **50:** 557–569.

Jiang, S., Fu, W., Chu, W., and Fuhrman, J.A. (2003) The vertical distribution and diversity of marine bacteriophage at a station off Southern California. *Microb Ecol* **45:** 399–410.

Kelly, C.K., Bowler, M.G., Pybus, O., and Harvey, P.H. (2008)

Phylogeny, niches, and relative abundance in natural communities. *Ecology* **89:** 962–970.
Krom, M.D., Kress, N., Brenner, S., and Gordon, L.I. (1991) Phosphorus limitation of primary productivity in the Eastern Mediterranean Sea. *Limnol Oceanogr* **36:** 424–432.
Leibold, M.A. (2008) Ecology: return of the niche. *Nature* **454:** 39–41.
Lewitus, A.J., and Kana, T.M. (1994) Responses of estuarine phytoplankton to exogenous glucose: stimulation versus inhibition of photosynthesis and respiration. *Limnol Oceanogr* **39:** 182–189.
Mantel, N. (1967) The detection of disease clustering and a generalized regression approach. *Cancer Res* **27:** 209–220.
Muyzer, G., de Waal, E.C., and Uitterlinden, A.G. (1993) Profiling of complex microbial populations by denaturing gradient gel electrophoresis analysis of polymerase chain reaction-amplified genes coding for 16S rRNA. *Appl Environ Microbiol* **59:** 695–700.
Muyzer, G., Brinkhoff, T., Nübel, N., Santegoeds, C., Schäfer, H., and Wawer, C. (1998) Denaturing gradient gel electrophoresis (DGGE) in microbial ecology. In *Molecular Microbial Ecology Manual*, Vol. 3.4.4. Akkermans, A.D.L., van Elsas, J.D., and de Bruijn, F.J. (eds). Dordrecht, the Netherlands: Kluwer Academic Publishers, pp. 1–27.
Øvreas, L., Bourne, D., Sandaa, R.A., Casamayor, E.O., Benlloch, S., Goddard, V., *et al.* (2003) Response of bacterial and viral communities to nutrient manipulations in seawater mesocosms. *Aquat Microb Ecol* **31:** 109–121.
Pinhassi, J., Gomez-Consarnau, L., Alonso-Sáez, L., Sala, M.M., Vidal, M., Pedrós-Alió, C., and Gasol, J.M. (2006) Seasonal changes in bacterioplankton nutrient limitation and their effects on bacterial community composition in the NW Mediterranean Sea. *Aquat Microb Ecol* **44:** 241–252.
Pradeep Ram, A.S., and Sime-Ngando, T. (2008) Functional responses of prokaryotes and viruses to grazer effects and nutrient additions in freshwater microcosms. *ISME J* **2:** 498–509.
Proctor, L.M., and Fuhrman, J.A. (1990) Viral mortality of marine-bacteria and cyanobacteria. *Nature* **343:** 60–62.
Proctor, L.M., and Fuhrman, J.A. (1992) Mortality of marine-bacteria in response to enrichments of the virus size fraction from seawater. *Mar Ecol Prog Ser* **87:** 283–293.
Riemann, L., and Middelboe, M. (2002) Stability of bacterial and viral community compositions in Danish coastal waters as depicted by DNA fingerprinting techniques. *Aquat Microb Ecol* **27:** 219–232.
Riemann, L.F., Steward, G., Fandino, L.B., Campbell, L., Landry, M.R., and Azam, F. (1999) Bacterial community composition during two consecutive NE Monsoon periods in the Arabian Sea studied by denaturing gradient gel electrophoresis (DGGE) of rRNA genes. *Deep Sea Res Part II* **46:** 1791–1811.
Sandaa, R.A., and Larsen, A. (2006) Seasonal variations in viral-host populations in Norwegian coastal waters: focusing on the cyanophage community infecting marine *Synechococcus* species. *Appl Environ Microbiol* **72:** 4610–4618.
Sandaa, R.A., Heldal, M., Castberg, T., Thyrhaug, R., and Bratbak, G. (2001) Isolation and characterization of two viruses with large genome size infecting *Chrysochromulina ericina* (*Prymnesiophyceae*) and *Pyramimonas orientalis* (*Prasinophyceae*). *Virology* **290:** 272–280.
Schwalbach, M.S., Hewson, I., and Fuhrman, J.A. (2004) Viral effects on bacterial community composition in marine plankton microcosms. *Aquat Microb Ecol* **34:** 117–127.
Selje, N., Simon, M., and Brinkhoff, T. (2004) A newly discovered *Roseobacter* cluster in temperate and polar oceans. *Nature* **427:** 445–448.
Sloan, W.T., Lunn, M., Woodcock, S., Head, I.M., Nee, S., and Curtis, T.P. (2006) Quantifying the roles of immigration and chance in shaping prokaryote community structure. *Environ Microbiol* **8:** 732–740.
Suttle, C.A. (1994) The significance of viruses to mortality in aquatic microbial communities. *Microb Ecol* **28:** 237–243.
Suttle, C.A. (2005) Viruses in the sea. *Nature* **437:** 356–361.
Suttle, C.A. (2007) Marine viruses – major players in the global ecosystem. *Nat Rev Microbiol* **5:** 801–812.
Suzuki, M.T., and Giovannoni, S.J. (1996) Bias caused by template annealing in the amplification of mixtures of 16S rRNA genes by PCR. *Appl Environ Microbiol* **62:** 625–630.
Tanaka, T., Henriksen, P., Lignell, R., Olli, K., Seppälä, J., Tamminen, T., and Thingstad, T.F. (2006) Specific affinity for phosphate uptake and specific alkaline phosphatase activity as diagnostic tools for detecting P-limited phytoplankton and bacteria. *Estuaries Coasts* **29:** 1226–1241.
Tanaka, T., Thingstad, T.F., Gasol, J.M., Cardelus, C., Jezbera, J., Sala, M.M., *et al.* Determine the ability of phosphate and glucose for bacteria in P-limited mesocmos of northwestern Mediterranean surface waters. *Aquat Microb Ecol* (in press).
Thingstad, T.F. (2000) Elements of a theory for the mechanisms controlling abundance, diversity, and biogeochemical role of lytic bacterial viruses in aquatic systems. *Limnol Oceanogr* **45:** 1320–1328.
Thingstad, T.F., and Lignell, R. (1997) Theoretical models for the control of bacterial growth rate, abundance, diversity and carbon demand. *Aquat Microb Ecol* **13:** 19–27.
Thingstad, T.F., Zweifel, U.L., and Rassoulzadegan, F. (1998) P limitation of heterotrophic bacteria and phytoplankton in the northwest Mediterranean. *Limnol Oceanogr* **43:** 88–94.
Van Etten, J.L., and Meints, R.H. (1999) Giant viruses infecting algae. *Annu Rev Microbiol* **53:** 447–494.
Van Wambeke, F., Christaki, U., Giannokourou, A., Moutin, T., and Souvemerzoglou, K. (2002) Longitudinal and vertical trends of bacterial limitation by phosphorus and carbon in the Mediterranean Sea. *Microb Ecol* **43:** 119–133.
Weinbauer, M.G., Christaki, U., Nedoma, A., and Simek, K. (2003) Comparing the effects of resource enrichment and grazing on viral production in a meso-eutrophic reservoir. *Aquat Microb Ecol* **31:** 137–144.
Winter, C., Smit, A., Herndl, G.J., and Weinbauer, M.G. (2004) Impact of virioplankton on archaeal and bacterial community richness as assessed in seawater batch cultures. *Appl Environ Microbiol* **70:** 804–813.
Wintzingerode, F., Goebel, U., and Stackerbrandt, E. (1997) Determination of microbial diversity in environmental samples: pitfalls of PCR-based rRNA analysis. *FEMS Microbiol Rev* **21:** 213–229.
Zhang, R., Weinbauer, M.G., and Qian, P.-Y. (2007) Viruses

and flagellates sustain apparent richness and reduce biomass accumulation of bacterioplankton in coastal marine waters. *Environ Microbiol* **9:** 3008–3018.

Supporting information

Additional Supporting Information may be found in the online version of this article:

Fig. S1. Development of pico- and nanoeukaryote abundance. Values given as mean and ranges of two parallel experiments.

Fig. S2. Development of *Synechococcus* abundance. Values given as mean and ranges of two parallel experiments.

Fig. S3. Numbers of different DGGE bands over time in the different treatments.

Please note: Wiley-Blackwell are not responsible for the content or functionality of any supporting materials supplied by the authors. Any queries (other than missing material) should be directed to the corresponding author for the article.